IRON METEORITE CANDIDATES WITHIN GALE CRATER, MARS, FROM MSL/MASTCAM MULTISPECTRAL OBSERVATIONS. D. F. Wellington (dfwellin@asu.edu)[1], J. R. Johnson[2], P.-Y. Meslin[3], J. F. Bell III[1], [1]Arizona State Univ., [2]Johns Hopkins Univ., APL, [3]IRAP, UPS-CNRS, Univ. Toulouse

Introduction: The Mastcam instruments on the MSL *Curiosity* rover each include an 8-position filter wheel that allows multispectral imaging in the wavelength range of 400-1100 nm [1,2]. The filter set captures broad electronic absorption bands that result, primarily, from the presence of Fe^{2+} and Fe^{3+} cations contained in constituent minerals and poorly crystalline phases of Gale Crater materials. Mastcam imaging observation commonly include loose float rock, which may have weathered out of the local bedrock or been transported from elsewhere. It is very commonly the case that the float material is a good spectral match to underlying or nearby bedrock; however, definite instances of spectral "erratics" in the Mastcam multispectral dataset can be found. Some of these rocks exhibit smooth, red-sloped reflectance spectra that are consistent with a composition rich in metallic iron [3]; we interpret these to be likely iron meteorites. Documenting these finds can provide information on meteorite fall statistics, physical weathering rates, and past environmental conditions within the crater (e.g., [4]).

These rocks are in addition to previously recognized iron meteorites within Gale Crater that include a cluster of meter-scale fragments designated Aeolis Palus 001-003 (formerly, "Littleton", "Lebanon", and "Lebanon-B") [5,6], smaller cm-size finds identified as Aeolis Mons 001-002 (previously "Egg Rock" and "Ames Knob") [6,7,8], and another recently observed small fragment informally known as "Mustards Island", identified by ChemCam as an iron meteorite. Chemical data were only acquired for the latter three fragments; for the candidate meteorites discussed below, Mastcam provides the only science instrument observations.

Observations: We have found that potential iron meteorites are often easily noticeable following standard image analysis techniques that are designed to enhance spectral differences in a multispectral sequence. This is because native martian materials commonly exhibit ferrous or ferric absorption features that are not present in unweathered meteoric iron. It is also possible to parameterize the spectral characteristics that distinguish iron-meteorite-like spectra from typical Gale Crater bedrock (as in [9]) and use quantitative measures, such as band ratios, to search the entire multispectral datset for image regions that are a spectral match. We have examined the Mastcam dataset thoroughly using both such techniques to identify rocks whose spectral properties are consistent with metallic iron, which we consider to provide good (although, without chemistry, not definitive) evidence for a meteorite interpretation. For dark-toned materials imaged in all or most filters, we consider a spectral profile that might yield a false positive to be likely uncommon. An example of such is manganese oxide, varieties of which may show smoothly increasing reflectance over the Mastcam spectral range (e.g., [10]); however, this and other such secondary phases would not necessarily be expected (nor have they been observed) to be abundant, or to uniformly cover the surface of a float rock. Greater potential for misidentification exists for observations that do not include the full Mastcam filter set, or for targets that are small or are covered by fewer pixels in the images; however, for the candidates presented here, we believe a metallic iron-rich composition is the most probable interpretation of the spectra.

Table 1: Candidate Iron Meteorite Fragments from MSL/Mastcam Multispectral Observations

Sol(s)	Number[1]	Size(s)[2]	Filters[3]
397	1	~ 6 cm	L1236
994-1032	8+	~ 3-5 cm	L0-6, R0-6[4]
1160	1	~ 5 cm	L0-6
1462-1463	2	~ 2-5 cm	L1236
1505[5]	1	~ 2 cm	L0-6
1512	1	~ 2 cm	L0-6
1610	1	~ 1 cm	L0-6
1819[6]	many	< 15 cm	R0-6

[1]When potential fragments grade in size down to the limit of the camera's resolution, an exact count is not possible. [2]Estimate is based on the longest axis and is approximate. [3]Band center wavelengths are 527-445-751-676-867-1012 nm (L1-6, left, M-34 camera) and 527-445-805-908-937-1013 nm (R1-6, right, M-100 camera); 0 is broadband RGB in each [1,2]. [4]Wavelength coverage varies by fragment. [5]Same FOV as Aeolis Mons 001, likely a pair. [6]Approx. 30 m from "Mustard Island", possibly paired.

A list showing the sol(s) and approximate number of iron meteorite fragments suggested by the spectral data is shown in Table 1. Spectral coverage varies from series of four-filter sequences intended for photometric analysis, to fragments captured by the wider field of view (FOV) of the M-34 (left, "L"), to those that could only be resolved in the M-100 (right, "R") images, to full-filter coverage (an observation acquired on sol 1032, originally noticed in a preceeding photometric sequence). The candidate meteorites are all relatively small (cm-sized); larger pieces or those close to the rover are more likely to be noticed by morphology in RGB Mastcam or engineering camera images, as was the case for previously recognized finds by this rover [5,7,8]. Aside from the Aeolis Palus cluster, however, those are also a few cm in scale, apparently a common size fraction. Clusters (several potential meteorites within a few meters, or tens of meters) appear to be common, with groups of two or more potentially linked fragments occurring approximately as often as single rocks. These likely formed from impact fragmentation or subsequent physical weathering; they are too close to have resulted from an atmospheric breakup. Unfortunately, the reflectance data are not sufficient to permit much speculation as to whether any of the widely separately clusters arose from the same impactor.

Each of these rocks shows a generally similar overall spectral shape; gradual, red-sloped, and distinct from both the mafic features that characterize the crater floor bedrock and oxidized layers of the Murray [11,12]. Mastcam spectra from each of the rocks or clusters listed in Table 1 are shown in Figure 1, together with several spectra from the confirmed or acknowledged meteorites mentioned in the introduction. In most cases, these fragments are too small to resolve finer details of their surfaces; for those that are, spectral varability across the surface is generally consistent with differences in illumination/viewing angles or dust coatings. Aeolis Mons 001 is an exception; spectrally distinct regions (see A and B spectra from different parts of the same rock, Figure 1) are consistent with mm-scale compositional differences that might arise from differing amounts of iron and nickel [3], the presence of minor iron oxidation products, or both.

All of these potential meteorites are interpreted as irons; our search for anomalous spectral signatures did not turn up any obvious chondrites. However, chondrites are harder to distinguish spectrally from native martian materials, and small pieces could have been overlooked. It is also possible that chondritic materials occur predominantly as a soil component (e.g., [13]) due to greater destruction on impact and/or higher susceptibility to physical weathering.

Conclusions and Future Work: Mastcam has acquired hundreds of multispectral sequences to date, which we have examined in detail to produce a list of candidate iron meteorite "finds" detected along the rover traverse. These data can be used for statistical analysis of the density of meteorites at this site, which can be compared against expectations of meteorite delivery, impact survival, and erosion rates (e.g., [14]), as well as counts from the MER rovers (e.g., [15,16]). We anticipate that Curiosity will continue to discover more examples as its mission continues.

References: [1] Bell, J.F., III *et al.* (2017) *Earth & Space Sci., 4*, 396. [2] Malin, M.C. *et al.* (2017) *Earth & Space Sci., 4,* 506. [3] Gaffey, M.J. (1976) *JGR 81,* 905. [4] Ashley, J.W. *et al.* (2011) *JGR 116*, E00F20. [5] Johnson, J.R. *et al.* (2014) *AGU Fall Mtg.*, #P51E-3989 [6] *Met. Bull. 106*, in prep. [7] Meslin, P.-Y. *et al.* (2017) *LPSC XLVIII*, 2258. [8] Wiens *et al.* (2017) *80th Mtg. Met. Soc.*, #6168. [9] Wellington, D.F. *et al.* (2017) *LPSC XLVIII*, 2885. [10] Arvidson, R.E. et al. (2016) *Am. Min. 101*, 1389. [11] Wellington, D.F. *et al.* (2017) *Am. Min. 102,* 1202. [12] Horgan, B. *et al.* (2017) *LPSC XLVIII*, 3021. [13] Yen, A.S. *et al.* (2006) *JGR 111*, E12S11. [14] Bland, P.A. and T.B. Smith (2000) *Icarus 144*, 21. [15] Schroder, C. *et al.* (2008) *JGR 113*, E06S22. [16] Johnson, J.R. *et al.* (2010) *LPSC XLI*, 1974.

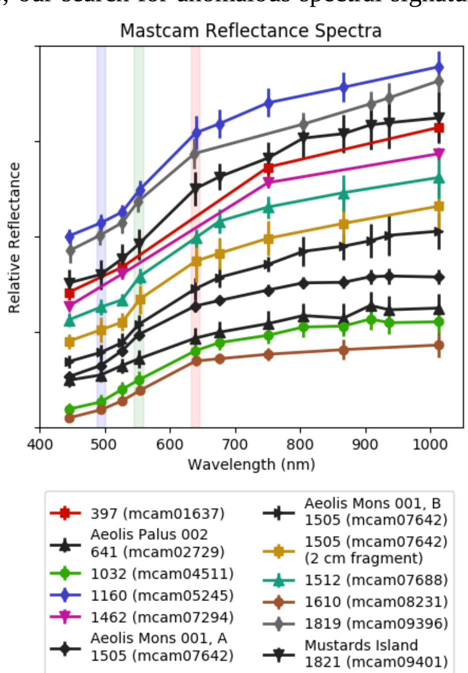

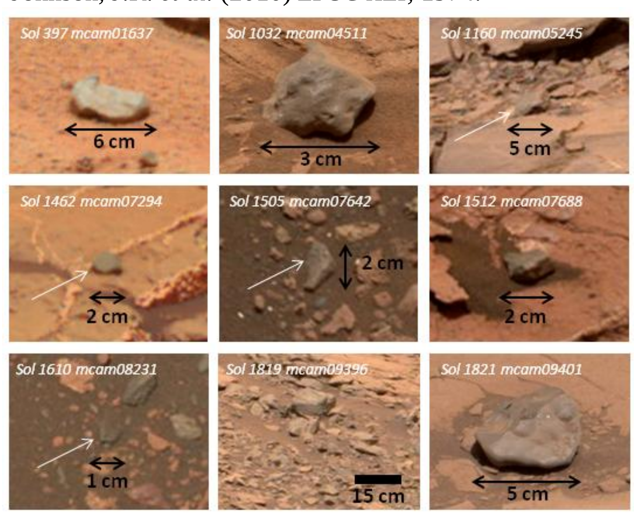

Figure 1: Left: Mastcam spectra from the candidate iron meteorites listed in Table 1 (for clusters, a spectrum from a single rock is given), offset for clarity; y-ticks are intervals of 0.1. Also shown are spectra from officially recognized meteorites and from the sol 1821 “Mustards Island” meteorite (black spectra). Top: Mastcam images of selected candidate meteorites, and “Mustards Island”. The sol 1819 example is a large cluster.